ISIJ International, Vol. 55 (2015), No. 10, pp. 2198–2205

Crystallographic Analysis of Lath Martensite in Ferrite-Martensite Dual Phase Steel Sheet Annealed after Cold-Rolling

Hiromi YOSHIDA,[1)]* Shusaku TAKAGI,[1)] Shota SAKAI,[2)] Shigekazu MORITO[2)] and Takuya OHBA[2)]

1) Steel Research Laboratory, JFE Steel Corporation, 1 Kokan-cho, Fukuyama, Hiroshima, 721-8510 Japan.
2) Department of Materials Science, Shimane University, 1060 Nishikawatsu-cho, Matsue, Shimane, 690-8504 Japan.

(*Received on September 28, 2014; accepted on June 12, 2015; originally published in Tetsu-to-Hagané, Vol. 99, 2013, No. 10, pp. 625–633*)

Cold-rolled and annealed ferrite-martensite dual phase (DP) steel sheets are useful for automotive applications because of their excellent balance of strength and elongation. Although martensite in ferrite-martensite DP steels has important roll in the mechanical properties, the crystallography and microstructure of lath martensite in DP steels have not been investigated in detail. In this paper, the crystallography and microstructure of lath martensite in a ferrite-martensite DP steel were studied using electron microscopy and electron diffraction analysis, and the crystallographic orientation relationship between the ferrite and martensite was analyzed. The main results are as follows: (1) The lath martensite in DP steels consists of some packets, each of which contains several blocks. This structure is the same as that of lath martensite in fully martensitic steels. (2) The common parallel close-packed plane of the martensite laths in a packet tend to be parallel to the close-packed plane of the adjacent ferrite grain, whose fraction is about 30%.

KEY WORDS: crystallography; lath martensite; dual phase steel; SEM/EBSD; orientation relationship between ferrite and martensite.

1. Introduction

The martensite steels produced by quenching and tempering has been used for machine structural use. Martensite in ferrite-martensite dual-phase steels (hereinafter, DP steels) also has important roll in strengthening of the automobile steel sheets. Therefore the importance of analyzing the microstructure and their mechanical properties of the martensite has been increased year by year.

Many researches of microstructure analyses of the martensite have been carried out.[1,2)] Especially in recent years, the microstructure and crystallography of martensite using electron back scatter diffraction (hereinafter, EBSD) were reported.[3)] Among several kinds of martensite morphologies, the lath martensite consisting of fine martensite crystals with a thickness of around 0.2 μm is frequently used in practical steels. **Figure 1** shows a schematic illustration of the microstructure of the lath martensite in low carbon steels. In the lath martensite structure, the grain boundaries of austenite are inherited invariably because of its diffusionless transformation characteristics, and the prior austenite grain is divided into packets, which are groups of laths having the same habit plane. A packet consists of several blocks, each of which in turn consists of groups of laths having similar crystal orientations.

However, previous researches on the martensitic microstructure described above concerned only fully martensitic steels and microstructural analysis of packets and blocks in DP steels has not been carried out. The less interest in martensite in DP steels is attributed to the view that the lath martensite is an undeformable and invariant hard phase. For example, Sugimoto *et al*.[4)] and Kurihara *et al*.[5)] discussed only the distribution morphology of martensite without the internal microstructure of the martensite.

On the other hand, Hasegawa *et al*.[6)] recently investigated the relationship between the volume fraction of martensite and its mechanical properties in DP steels, and showed that the plastic strain of martensite increases with the increase in martensite fractions. Ueji *et al*.[7)] also showed that the groups of the laths in the martensite deformed nonuniformly under the plastic strain. As far as fracture behavior is concerned, it has been shown that martensite in DP steels is deformed and thereby affects fracture behaviors.[8)] Voids are generated at the ferrite-martensite interface, and these voids

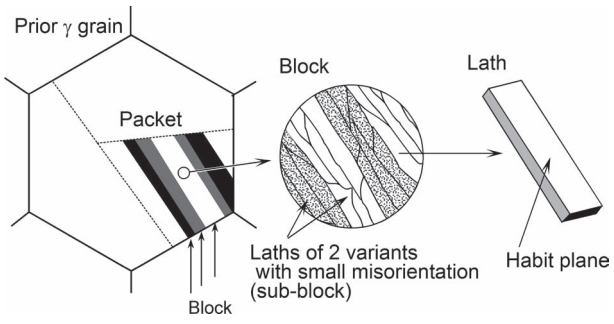

Fig. 1. Schematic illustration showing the microstructure of lath martensite in low carbon steels.

* Corresponding author: E-mail: hirom-yoshida@jfe-steel.co.jp
DOI: http://dx.doi.org/10.2355/isijinternational.ISIJINT-2014-641

cause fracture by coalescing.[9] Sato *et al*.[10] investigated the relationship between the three-dimensional morphology of martensite and the locations where void formation occurs around the fracture area in DP steels, and suggested that voids generated at necks in martensite. Thereby, the mechanical properties of DP steels might be improved further by clarifying the microstructure of martensite and controlling the crystallographic orientation relationship of ferrite and martensite in DP steels.

Sakai *et al*.[11,12] clarified the crystallography of martensite in the hot-rolled and annealed DP steel. However, cold rolling is usually performed after hot rolling to obtain a target thickness, surface qualities and so on to produce practical steel sheets. Therefore, the purposes of the present research are to investigate martensite structures in DP steels, which are cold-rolled and annealed, compared to that in martensitic steels especially focusing crystallographic relationship between ferrite and martensite.

2. Experimental Procedure

2.1. Chemical Composition and Heat Treatments of Specimens

The chemical composition of the steel vacuum melted steel is shown in **Table 1**. **Figure 2** shows the rolling conditions and thermal history of the specimens. Soaking temperature was 1 523 K, and hot rolling was carried out in the temperature range of austenite, followed by cooling to room temperature. The thickness of the hot-rolled (hereinafter, HR) steel was 5 mm. Both side of the HR sheet was ground to get a thickness of 4 mm and rolled to a thickness of 2 mm by cold rolling. The sheet was then annealed at 1 053 K in intercritical region for 1.2 ks in a salt bath followed by water quenching to obtain specimens consisting of ferrite-martensite dual phase (hereinafter, denoted as CA steels).

2.2. Microstructure Analysis Method

The samples were cut perpendicular to the rolling and normal directions of the sheet, and were observed on the transverse cross section shown in **Fig. 3**. The specimens were mechanically polished using abrasive paper and an alumina suspension, followed by buffed with colloidal silica. The polished surface was etched with a 3% nitric acid-alcohol (3%-nital) solution and observed using an optical microscope. Microstructural observation and crystal orientation analysis were performed by scanning electron microscope/electron back scatter diffraction (JEOL JSM 7001FA/EDAX-TSL OIM Ver. 5.3; hereinafter, SEM/EBSD) and a transmission electron microscope (JEOL JEM-2010; hereinafter, TEM) at around the 1/4 thickness position of the section.

Table 1. Chemical composition of the steel used (mass%).

C	Si	Mn	P	S	Al	N
0.13	1.5	2.0	0.01	0.001	0.03	0.004

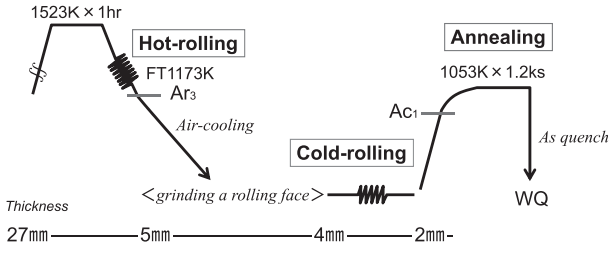

Fig. 2. Rolling conditions and heat treatment history of the specimens.

It is well known that the multiple microstructural units of lath martensite steels have a hierarchical structure.[3,13] The unit called a packet is considered to comprise "a group of laths having similar habit planes". From the crystallography, a packet can be considered "a group of laths having the same close-packed plane parallel relationship with the austenite matrix". The blocks which exist in a packet are defined as groups of laths having a similar crystal orientation. The block boundary is a high angle grain boundary whose misorientation angle is around 60°. Because the CA specimen used in this research had a fine ferrite-martensite microstructure, as shown in **Fig. 4**, it was difficult to observe packets by optical microscopy. Therefore, identification of both packets and blocks was performed by using SEM/EBSD.

Crystallographically, the laths contained in each packet of martensite have the same close-packed plane parallel relationship with the austenite matrix. The Kurdjumov-Sachs orientation relationship (hereinafter, K-S relationship) assumes that the lath $(011)_M$ common close-packed plane and that $[\bar{1}\,\bar{1}\,1]_M$ close-packed direction are parallel to the prior austenite $(111)_A$ close-packed plane and that $[\bar{1}01]_A$ close-packed direction. Having common close-packed planes in the $\{001\}_M$ and $\{011\}_M$ pole figures are identified as a packet (Hereinafter, pole figures are referred to as PF, and the subscripts A, M, and F mean austenite, martensite, and ferrite, respectively). We estimated the blocks and their boundaries as the measured regions with misorientation angles within 5° in one packet, and high angle grain boundaries of around 50–60°, respectively. The estimation, *i.e.* misorientation angle within 5°, is determined to identify the packet boundaries because the smallest misorientation angle between different packets is 10.5°, and the

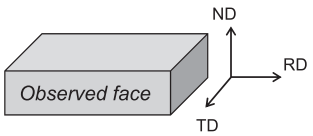

Fig. 3. Schematic illustration showing observed face of the specimens.

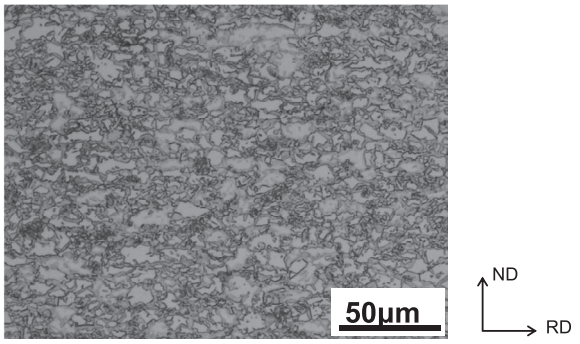

Fig. 4. Optical micrograph of the CA specimen etched with a 3%-nital. The specimen contains martensite regions (gray) and ferrite regions (white). The ferrite grain boundaries are not smooth.

misorientation angle in single variants is considered to be roughly within 5°.[14] In the case of low carbon steels, two variants with a misorientation of 10.5° exist in one packet. These types of laths are crystallographically different from each other and the groups of laths are called sub-blocks.[3] Sub-blocks were not identified in the analyses in the present study.

The prior austenite region and packet size was measured using image processing software (Olympus analySIS FIVE), and the square root of the average area value was defined to be the nominal grain size. In measurement of the block thickness t, the normal vector of the common close-packed plane of the different lath variants in a packet was obtained from the crystallographic orientation data by SEM/EBSD measurements, and a projection line of the normal vector was drawn on an orientation image map that used the same data, after which the number n of block boundaries that crossed a projector of length L was counted. Assuming the angle between the specimen plane-normal and the normal vector of a common close-packed plane is θ, the block thickness t can be expressed by Eq. (1):

$$t = L \times \sin\theta / n \quad \cdots\cdots\cdots\cdots\cdots\cdots (1)$$

Packets in which θ was larger than 40° were selected, and the block thicknesses were calculated under the condition that L was within the packet.

3. Results

3.1. Microstructure of CA Specimen

Figure 4 shows the optical micrograph of the CA specimen. The CA specimen consisted of ferrite and martensite. The area ratio of the ferrite is 44%. The ferrite microstructure elongated toward the rolling direction and had concave or convex interface. The nominal grain size of ferrite was 4 μm. On the other hand, large and fine martensite regions were observed as a morphology penetrating into the ferrite grains, and some martensite regions existed in ferrite grains. The coarse regions are similar size to the ferrite regions, and the fine regions have narrow shape with a few μm thickness.

The results of the SEM/EBSD analysis of the CA specimens are shown in **Fig. 5**. Figures 5(a) and 5(b) show the SEM image and corresponding image quality (IQ) map, respectively. Figure 5(c) is a magnified view of the white square area in Fig. 5(b). Figure 5(c) shows two packets, Packet-1 and -2, and Fig. 5(d) shows Packet-1 with each block represented by a different color. These images indicate that the martensite is also made up of multiple individual packets. The colored IQ maps such as Fig. 5(d) show that the packets consist of one or some blocks. Figures 5(e) and 5(f) are $\{001\}_M$ PF and $\{011\}_M$ PF of Packet-1, respectively. The colors in the figures correspond to the blocks in Fig. 5(d). These blocks in martensite packets have the common closed-packed plane parallel relationship with austenite and the misorientation angle between the blocks is approximately 60°.These results indicate the fact that the martensite in DP steels also has the same substructure as the martensite in martensitic steels.

The microstructure was observed by using TEM. **Figures 6**(a) and 6(b) show a bright field image of a CA specimen and the electron diffraction pattern, respectively. The arrows

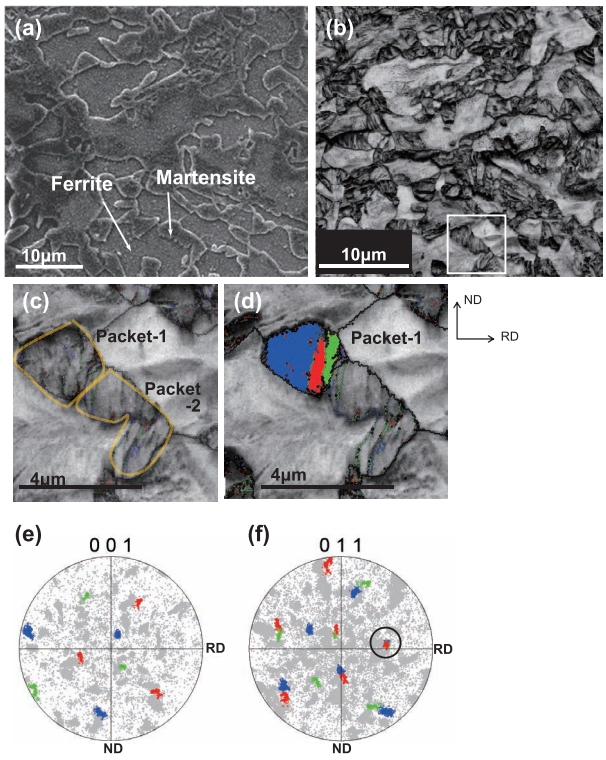

Fig. 5. (a) SEM image, (b) image quality map, (c) magnified view of the white square in (b), (d) block map of Packet-1 with image quality data, (e) $\{001\}_M$ pole figure and (f) $\{011\}_M$ pole figure of a CA specimen.

in Fig. 6(a) indicate a lath and its thickness. The thickness of the laths in the CA specimens is in the range from 100 to 200 nm, which is similar to the thickness of the martensite laths in ordinary low carbon steels.[2] In Fig. 6(b), the laths have different types of crystal orientations having common $(011)_M$ diffractions in martensite regions, with parallel laths indicated by the yellow lines in Fig. 6(a), and the common diffractions correspond to the normal directions of the habit planes of the laths. The habit planes were identified using trace analyses. These observations show that the regions indicated by the yellow lines in Fig. 6(a) were packets with blocks. The diffraction shown by the sky-blue arrow in Fig. 6(b) is the $(\bar{1}\,1\,\bar{1})_A$ of austenite and was suggested the existence of film-shaped residual austenite with martensite as in martensitic steels. Moreover, the fine martensite surrounded by ferrite grains in Fig. 6(a), contains only one packet along the thickness direction of the maetensite region and the packet morphology was equiaxed. In other words, the thickness of the martensite regions corresponds to the prior austenite grains and packet size.

Next, the block thickness was investigated. The CA specimens have coarse and fine martensite regions. For example, the regions A and B shown in **Fig. 7** have fine martensite regions, and region C has coarse one. The prior austenite grain sizes in the coarse and fine regions are 7 μm and 2 μm, respectively. Furthermore, the thickness of the blocks in the coarse and fine regions is 0.65 and 0.46 μm, respectively. The tendency of the block thickness was confirmed from distribution of the block thickness, more than 30 points. It means that the block thickness decreases with decreasing the prior austenite grain size. This is the same tendency as the results reported by Morito *et al.*[15] for low carbon martensitic steels and by Sakai *et al.*[12] for the DP steel produced

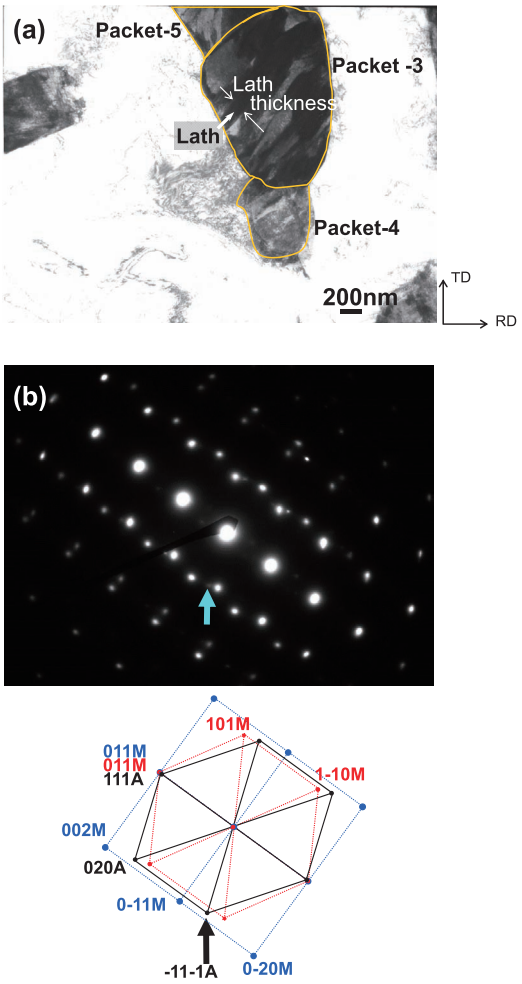

Fig. 6. (a) Bright field TEM image of a CA specimen showing the structure of martensite consisting of several packets, (b) electron diffraction pattern taken from Packet-3. The sky-blue and black arrows indicate $(\bar{1}1\bar{1})_A$.

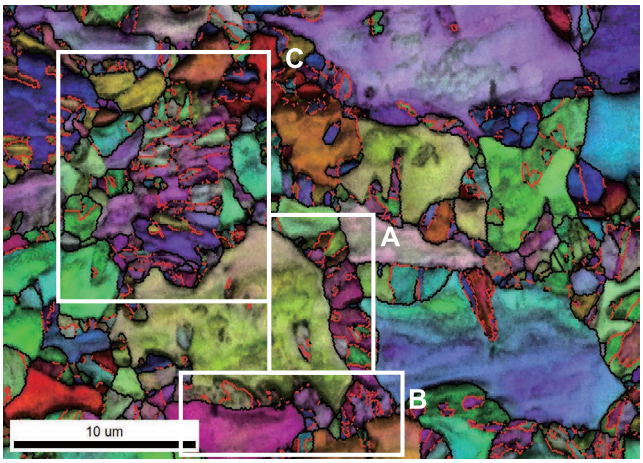

Fig. 7. Orientation image map with image quality data of a CA specimen showing analysis areas A, B, and C. Bold red and black lines indicate block and the other high angle grain boundaries, respectively.

by hot rolling and annealing.

3.2. Orientation Relationship between Ferrite and Martensite

It is well known that lath martensite start to forms from austenite grain boundaries,[16] and in the case of a martensitic steel, it has been reported that a martensite variant selection rule exists due to the constraint caused by the austenite grain boundary and the crystallographic orientation between the austenite grains.[17] On the other hand, Sakai *et al.*[11,12] carried out an analysis of the martensite microstructure in the DP steel and the orientation relationship between ferrite and martensite in HR specimens and annealed specimens after hot rolling (hereinafter, hot-rolled and annealed; HRA specimens). The results revealed there was a close-packed plane parallel relationship between the $\{110\}_M$ common close-packed planes of martensite blocks in the martensite packets, *i.e.* the habit planes of martensite laths, and the $\{110\}_F$ planes of adjacent ferrite grains. This result suggested that the crystallographic orientation of martensite in DP steels is affected by that of adjacent ferrite grains. Then, the orientation relationship between the martensite and adjacent ferrite in the CA specimen was investigated in order to clarify the effect of ferrite on the crystallographic orientation of the martensite that forms during cooling after intercritical annealing. The plane parallel relationship between the common close-packed plane of the martensite packet and the close-packed plane of one of the adjacent ferrite grains was confirmed from the $\{001\}_M$ PF and $\{011\}_M$ PF. Usually, the prior austenite grains are able to be identified in order to clarify the orientation relationships of martensites. In the CA specimen, it was difficult to identify all the prior austenite grains because of the fine ferrite-martensite microstructure. Thus, martensite packet was determined as unit structure of martensite in this investigation. When the misorientation angle between the common close-packed plane $\{011\}_M$ of the martensite packets and the close-packed plane $\{011\}_F$ of the adjacent ferrite is within 5°, it was judged that "a parallel relationship exists between the common close-packed plane of the martensite packet and the close-packed plane of the ferrite". This analysis method was applied to all measurable packets, and the ratio of the parallel relationship packets and adjacent ferrite grains was calculated by dividing the number of packets having the parallel relationship with adjacent ferrite by the total number of analyzed packets. The judgment criteria for the method were determined based on the fact that misorientation angles between martensite laths in a sub block was within 5° in most cases.[14] **Figure 8** shows the analyses of Packet-2 in Fig. 5. The black circle in the $\{011\}_M$ PF shows the common close-packed plane of Packet-2, which is shown by the white circle in the Fig. 8(a). It is confirmed that the common close-packed planes of Packet-2 are parallel to the close-packed plane of the adjacent ferrite (shown in blue). However, in Packet-1, this close-packed plane parallel relationship was not observed with any of the ferrite grains. As a distinctive feature of the CA specimen, multiple fine martensite grains exist in the area around a large ferrite grain. The martensite existing around large ferrite was analyzed. Moreover, in **Fig. 9**, the common close-packed planes of Packet-6 are parallel to the close-packed plane of the adjacent ferrite (shown in green). However, in Packet-7 which has island-like shape, this close-packed plane parallel relationship was not observed with the adjacent ferrite grain (shown in green). In the martensite packets that existed in isolation within ferrite grains, as Packet-7, a tendency not

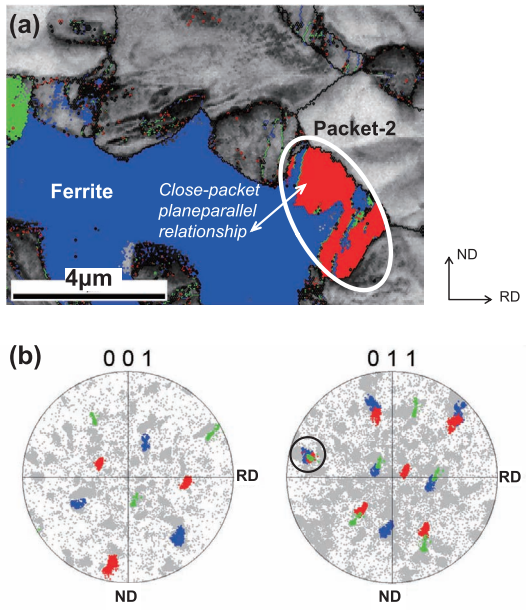

Fig. 8. (a) Orientation image map with image quality data, (b) $\{001\}_M$ and $\{011\}_M$ pole figures of Packet-2 and ferrite in a CA specimen. Packet-2 has a close-packed plane parallel relationship with the adjacent ferrite grain.

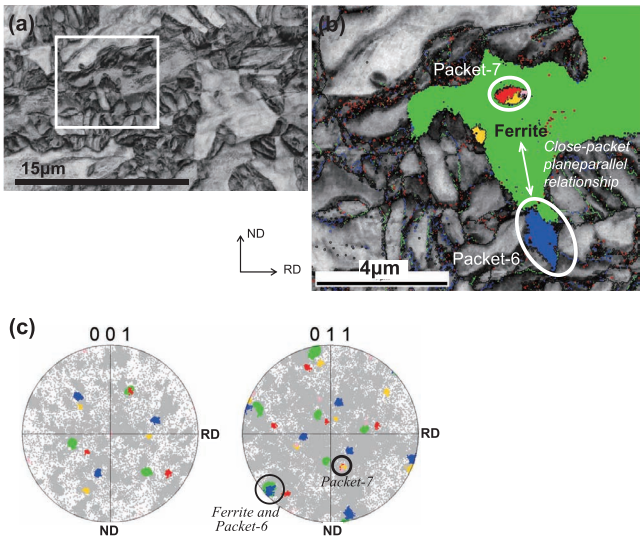

Fig. 9. (a) Image quality map, (b) orientation image map with image quality data, which is a magnified view of the area enclosed by the box in (a), and (c) $\{001\}_M$ and $\{011\}_M$ pole figures of Packets-6 and -7 and ferrite in a CA specimen. Packet-7, which has an island-like shape, does not have a close-packed plane parallel relationship with the surrounding ferrite.

to have a close-packed plane parallel relationship with the surrounding ferrite was observed.

As a result of these analyses, it was found that about 30% of martensite packets had a close-packed plane parallel relationship with the adjacent ferrite. Because the percentage of martensite packets and adjacent ferrite pairs which had the close-packed plane parallel relationship was 40% in hot-rolled and annealed materials,[11,12] the close-packed plane parallel relationship between the martensite packets and their adjacent ferrite grains in the CA material is a little weak in comparison with hot-rolled and annealed materials.

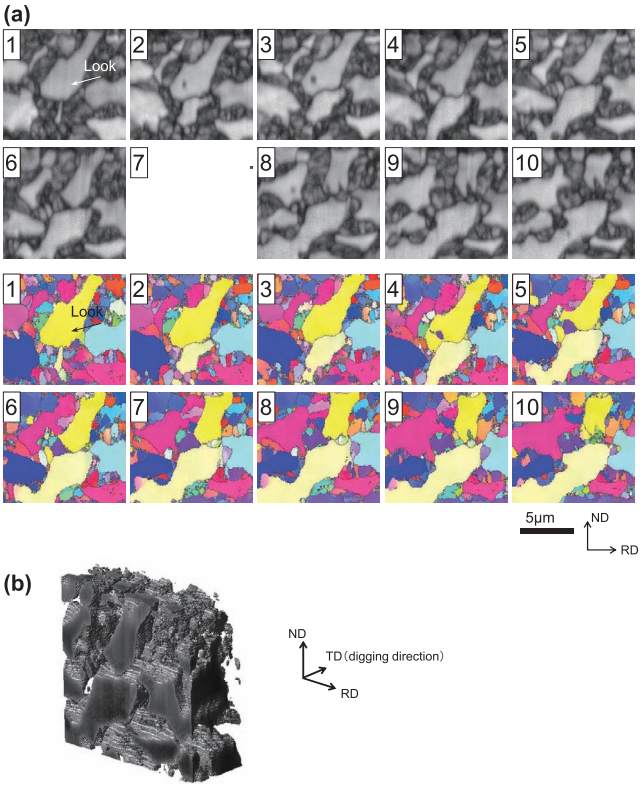

Fig. 10. (a) Image quality map (upper line) and orientation image map (lower line) in a CA specimen. (b) stereogram in which figures No. 1–10 are overlaid sequentially.

3.3. Three-dimensional Microstructural Observation of a DP Steel

In a two-dimensional view, as shown in Fig. 4, the microstructure of the DP steel consists of fine grains with complex shapes, and some martensite packets existing in apparent isolation within a ferrite grain was observed as shown in Fig. 9. However, there is a possibility that this martensite may adjoin other surrounding ferrite grains in three-dimension. Therefore, to reveal the 3D distribution of surrounding ferrite grains after mechanically polishing the CA specimen with a colloidal silica suspension, the specimen repeatedly removed along the TD in steps of 0.2 μm by focused ion beam (FIB) processing, and continuous SEM/EBSD observation was performed down to the depth of 20 μm. FIB was performed under conditions of 30 kV and 3 nA using Ga ions. An FEI Quanta 3D 200 instrument was employed in the microstructural observations using EBSD measurements.

An example of the observation results is shown in **Fig. 10**. The upper 10 figures in Fig. 10(a) show the IQ maps, and the lower 10 figures show the corresponding orientation image maps. Focusing on the yellow-colored ferrite shown by the arrow in the orientation image map No. 1 and digging down under this view, a region with a different orientation (purple) appears in this ferrite in the view in No. 4. In the IQ map, this purple region corresponds to the dark region, *i.e.* a low IQ value region and thus, is martensite. In No. 2 and 3, where the purple martensite region is not observed, the area with low IQ values has already appeared at the same position. This shows that the yellow ferrite receives plastic deformation locally by the formation of the purple martensite. Deeper into the specimen, the shape of the

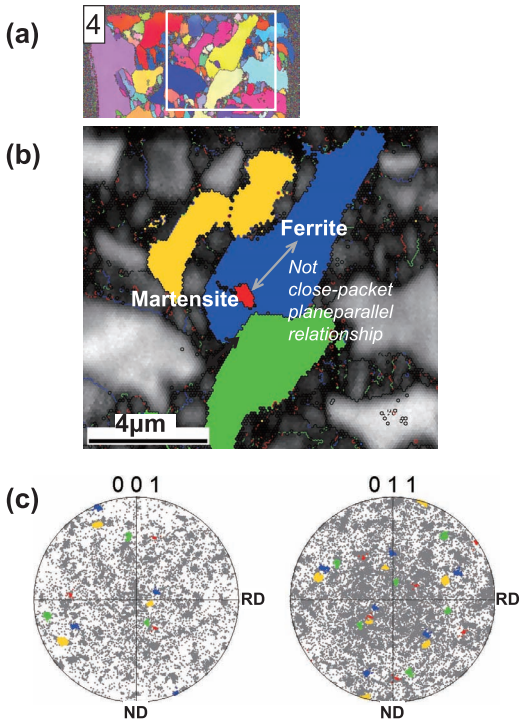

Fig. 11. (a) No. 4 orientation image map of Fig. 10, (b) orientation image map with image quality data, which is a magnified view of the square in (a), (c) $\{001\}_M$ and $\{011\}_M$ pole figures showing that a close-packed plane parallel relationship does not exist between the martensite (red) and ferrite (blue) indicated by the double-headed arrow.

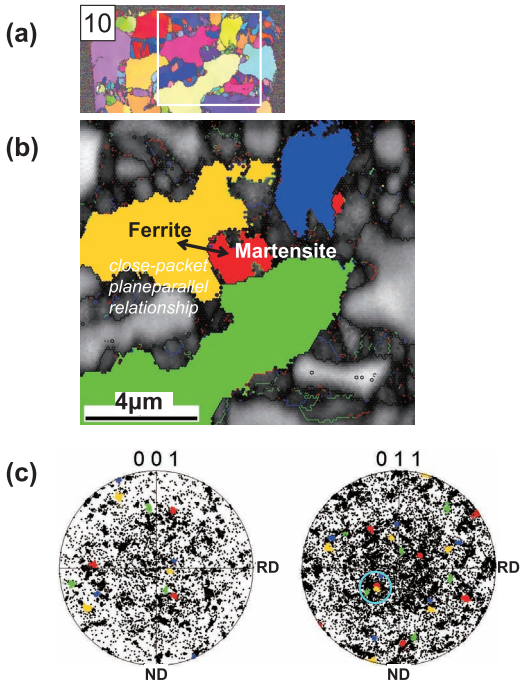

Fig. 12. (a) No. 10 orientation image map of Fig. 10, (b) orientation image map with image quality data, which is a magnified view of the square in (a), (c) $\{001\}_M$ and $\{011\}_M$ pole figures showing that a close-packed plane parallel relationship exists between the martensite (red) and ferrite (yellow) indicated by the double-headed arrow.

ferrite grains changes, and the martensite region becomes larger also and appears to be adjoining surrounding ferrite grains. The yellow ferrite and the island-like purple martensite that appears in the ferrite in orientation image map No. 4 join with another pink-colored ferrite grain at the position in No. 10. This result revealed that the island-like martensite regions which apparently exist in isolation from ferrite grains in the two-dimensional observations actually attach to adjacent ferrite grains in three dimensions. The three-dimensional morphology of ferrite and martensite reconstructed from Fig. 10(a) is shown in Fig. 10(b). The microstructures of the DP steel, which had a complex shape in the two-dimensional view, also became extremely complex when viewed three-dimensionally.

Next, the orientation relationship of this purple martensite with the surrounding ferrite was analyzed. As a result, as shown in **Fig. 11**, the yellow ferrite in view No. 4 of Fig. 10 and the purple martensite which appeared in island form in that ferrite do not have a close-packed plane parallel relationship, but in the view No. 10 of Fig. 10, the purple martensite has a close-packed plane parallel relationship with the adjacent pink ferrite, as shown in **Fig. 12**. From this result, the martensite that exists in isolation in ferrite grains in a two-dimensional view also adjoins other ferrite grains three-dimensionally, and can have a close-packed plane parallel relationship with the adjacent ferrite.

4. Discussion

4.1. Effect of Microstructure on Prior Austenite Grain Size and Block Thickness

In a single-phase martensite microstructure, it is known that changes in the block thickness depend on the prior austenite grain size and carbon content. In Chapter 3, the results of the present research show the same tendency of the relationship between the prior austenite grain size and the block thickness as that described in previous reports such as Morito *et al.*[15] and Sakai *et al.*[12] The results, which were measured in the papers above, are summarized in **Table 2**, and the effect of the prior austenite grain size on the block thickness of martensite is shown in **Fig. 13**. The effect of the prior austenite grain size on the block thickness of martensite is different in martensitic and DP steels. At the same prior austenite grain size, the block thickness of martensite in DP steels was smaller than that in martensitic steels. According to the results reported by Morito *et al.*,[15] the relationship between block thickness t [μm] and prior austenite grain size d_A [μm] in Fe-0.2%C-2%Mn steel is expressed as Eq. (2):

$$t = 0.006 \times d_A + 1.08\ [\mu\mathrm{m}] \quad \ldots\ldots (2)$$

On the other hand, in DP steels, the relationship between block thickness and prior austenite grain size d_A in CA and the hot-rolled and annealed specimens[12] is expressed as Eq. (3):

$$t = 0.022 \times d_A + 0.48\ [\mu\mathrm{m}] \quad \ldots\ldots (3)$$

From the slopes of these equations in comparison with martensitic steels, the block thickness in DP steels rapidly decreases with decreasing prior austenite grain size. One of the reasons for this difference is the difference in the chemical compositions of the steels used by Morito *et al.*[15] and that used in this research. The specimen used by Morito *et al.*[15] was Fe-0.2%C-2%Mn, whereas that used

Table 2. Relationship between prior austenite (γ) grain size and block thickness in Fe–C–Mn alloys. (Chemical compositions of materials: this study and Sakai *et al.*:[12] Fe-0.13C-2Mn, Morito *et al.*:[15] Fe-0.2C-2Mn).

Structure	Dual phase				Single phase				
Study	This study		Sakai *et al.*		Morito *et al.*				
Prior γ grain size [μm]	2	7	2.7	19	6.3	14.6	55	190	349
Block thickness [μm]	0.46	0.65	0.6	0.9	1.0	1.2	1.7	2.0	3.4

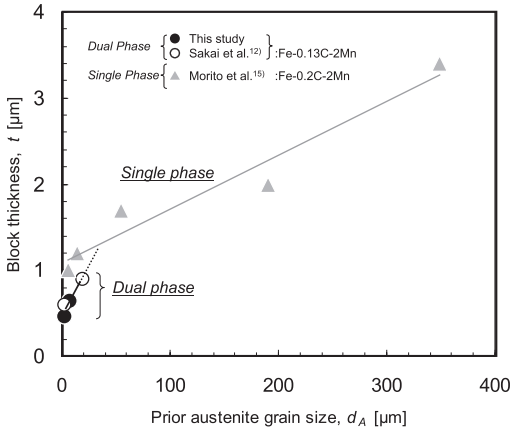

Fig. 13. Relationship between prior austenite (γ) grain size and block thickness in Fe–C–Mn alloys.

in the present research was Fe-0.13%C-2%Mn-1.5%Si, as shown in Table 1. In the DP steel, the carbon content of the martensite is different from the average content of the DP steel due to element partition during intercritical annealing. When simply calculated from the volume fraction of ferrite and martensite by the lever relation, which is 44:56, the carbon composition of the martensite in the CA specimen is estimated to be 0.23 mass%. Otherwise, the carbon, Si and Mn composition of the prior austenite in the CA specimen are estimated with calculation using Thermo-Calc. As for the volume fraction of ferrite and martensite, carbon, Si and Mn contents in the austenite are 0.23%, 1.4% and 2.6% respectively. Toji *et al.*[18] investigated microstructures using the same composition as in the present study annealed at 1 073 K in the intercritical temperature region. The paper showed that, in annealing for 1 000 s, Mn was enriched to approximately 2.5% in the austenite. Thus, the carbon content is approximately the same as that of the low carbon steels used by Morito *et al.*[15] Maki *et al.*[19] investigated the influence of alloying elements on packet size and concluded that alloying elements other than C do not have a large effect on the size of packets. From the report the distribution of the concentrations of alloying elements in the specimens used in this research and the difference of the present specimens from those used by Morito *et al.*[15] have a little effect on the relationship between block thickness and prior austenite grain size.

Another possible explanation of the difference is the influence of irregularity of the austenite-ferrite interphase boundaries on the block thickness. As shown in Figs. 4 and 11, the microstructure of the CA specimen is complicated. From the results reported by Sakai *et al.*,[12] the HRA specimens have more complex morphologies than those of the HR specimens. In general, martensite laths appear from austenite grain boundaries according to variant selection rules.[20] Thus, the formation of martensite blocks is determined by the crystallographic condition and nature of the grain boundary. In the CA specimen, ferrite exists around the austenite grains and the austenite-ferrite interfaces are not smooth. Therefore, the constraint for block formation will be different from that in martensitic steels, and the tendency of the relationship between block thickness and prior austenite grain size will also be different in martensitic and DP steels.

The reasons for the complex morphology in the CA specimen are discussed as follows. The specimens in the DP steel used by Sakai *et al.*[12] were annealed at intercritical temperature after hot rolling. Austenite grains were formed from bainite and/or retained austenite included in the bainite during annealing in the ferrite-austenite intercritical region. On the other hand, the CA specimen in the present research was obtained by cold rolling and annealing. Therefore, the fine austenite grains formed from recovered/recrystallized or nonrecrystallized ferrite regions during annealing. The austenite grains are finer than those in the hot-rolled and annealed specimens because the number of nucleation sites of austenite in the CA specimen is larger than that in the HRA specimens. Furthermore, in the CA specimen, recovery and recrystallization of ferrite occur during annealing simultaneously with austenite generation. As a result, local irregularities caused by recovery/recrystallization of ferrite appear at the ferrite-austenite interface.

4.2. Orientation Relationship of Ferrite and Martensite

The reason why the ratio of the close-packed plane parallel relationship between ferrite and martensite in the CA specimen is lower than that in the hot-rolled and annealed specimen will be discussed.

First, the effect of cold rolling/recrystallization is conceivable, as follows: The austenite grains have the K-S orientation relationship with adjacent ferrite grains during intercritical annealing. During annealing, recovery and recrystallization of deformed ferrite occur, and deviation of the crystallographic orientation in the ferrite grains appears. Considering this, the crystallographic orientation relationship between ferrite and austenite can deviate from the K-S relationship because of the change in orientations of ferrite by recrystallization. For example, the green colored points in $\{001\}_M$ and $\{011\}_M$ PFs in Fig. 9 show relatively large scattering in crystallographic orientation within a single ferrite grain. In contrast, the dispersion of crystallographic orientations within a single ferrite grain was not particularly noticeable in the HRA specimen used by Sakai *et al.*[12] From the colored orientation image with the gray-scaled IQ map in Fig. 7, color gradations can be seen in the coarse ferrite grains, indicating that the crystallographic orientations in the ferrite grains are not uniform, and possible residual deformation remains, as indicated by black-to-gray regions with low IQ value. The influence of dislocations introduced in ferrite by cold rolling cannot be ignored, and this kind of orientation scattering in the ferrite grains is a distinctive feature of the CA specimen.

A second possibility is the limitation of the two-dimen-

sional observations. Figure 10 shows that the martensite packets which exist in isolation from ferrite grains in the two-dimensional observations actually adjoin other ferrite grains three-dimensionally; this is attributed to the fact that the ferrite-austenite microstructure in the CA specimen becomes fine and complex during intercritical annealing, as discussed above. Furthermore, Fig. 12 shows that a close-packed plane parallel relationship exists between martensite packets and the ferrite grains which they adjoin three-dimensionally. That is, even in case a close-packed plane parallel relationship does not exist between martensite and the adjacent ferrite in a two-dimensional view of a certain cross section, there are cases in which a close-packed plane parallel relationship exists with a ferrite grain that adjoins the martensite three-dimensionally. In the present study, it is difficult to identify the orientation relationships between martensite and adjacent ferrite in two-dimensional observations because the microstructure of the CA specimen is finer and more complex than that of the HRA material used by Sakai *et al*.[12] The exact ratio of the close-packed plane parallel relationship existing in CA materials may be higher than that measured in this research.

Sato *et al*.[21] performed three-dimensional observations of martensite regions in DP steels, and showed that martensite takes various morphologies depending on the annealing conditions. Thus, for crystallographic microstructure analyses of high strength cold-rolled steels such as DP steels which have fine and complex grained microstructures, it is necessary to apply three-dimensional observations for identification of the orientation relationship between martensite and ferrite grains.

5. Conclusion

Martensite microstructures in DP steels were measured and compared with that in fully martensitic steels, and the crystallographic relationship between ferrite and martensite was investigated. The results obtained are as follows.

(1) The martensite in the DP steels consists of packets and blocks in the same manner as the martensitic steels.

(2) The ratio of the parallel relationship between the common close-packed planes of the martensite packets and the {110} planes of ferrite grains is about 30% which is smaller than that in hot-rolled and annealed specimens previously reported. One reason for this difference is that the orientation relationship between the ferrite and austenite regions before quenching deviates from the K-S orientation relationship due to recovering and/or recrystallization of ferrite during annealing. In addition, even though the close-packed plane parallel relationship between martensite packets and ferrite grains could not be observed by two-dimensional observations, a close-packed plane parallel relationship between martensite packets and other ferrite grains adjoining that martensite three-dimensionally is considered possible. To identify the microstructures and crystal orientation relationships correctly, it is necessary to observe the microstructure not only two-dimensionally, but also three-dimensionally.

(3) In DP steels produced by cold rolling and annealing after hot rolling, the martensite block thickness is smaller than that in martensitic steels. One of the reasons for this tendency is the numerous irregularities of the austenite-ferrite interphase boundaries caused by annealing of the cold-rolled microstructure.

Acknowledgement

S. M. (Shimane University) wishes to express his thanks for partial support by the Inter-University Cooperative Research Program of the Institute for Materials Research, Tohoku University (Proposal No. 08K0095, 09K0016).

REFERENCES

1) G. Krauss: *Mater. Sci. Eng. A*, **273**–**275** (1999), 40.
2) Z. Nishiyama: Martensitic Transformation, Maruzen, Tokyo, (1979).
3) S. Morito, H. Tanaka, R. Konishi, T. Furuhara and T. Maki: *Acta Mater.*, **51** (2003), 1789.
4) K. Sugimoto, T. Sakaki, T. Fukusato and O. Miyagawa: *Tetsu-to-Hagané*, **71** (1985), 994.
5) K. Kurihara, Y. Hosoya and K. Nakaoka: *Tetsu-to-Hagané*, **68** (1982), 1195.
6) K. Hasegawa, Y. Toji, H. Minami, H. Ikeda, T. Morikawa and K. Higashida: *Tetsu-to-Hagané*, **98** (2012), 320.
7) R. Ueji, N. Tsuji, Y. Minamino and Y. Koizumi: *Acta Mater.*, **50** (2002), 4177.
8) M. Kurita, K. Sotoyama, S. Nomura and K. Kunishige: *Tetsu-to-Hagané*, **81** (1995), 1091.
9) D. Kondo, K. Kunishige and R. Ueji: *Tetsu-to-Hagané*, **92** (2006), 457.
10) N. Sato, M. Ojima, Y. Tomota and Y. Adachi: *CAMP-ISIJ*, **24** (2011), 1029, CD-ROM.
11) S. Sakai, S. Morito, T. Ohba, H. Yoshida and S. Takagi: *CAMP-ISIJ*, **22** (2009), 153, CD-ROM.
12) S. Sakai, S. Morito, T. Ohba, H. Yoshida and S. Takagi: *Netsu Shori*, **51** (2011), 233.
13) S. Morito, H. Saito, T. Ogawa, T. Furuhara and T. Maki: *ISIJ Int.*, **45** (2005), 91.
14) S. Morito, X. Huang, T. Furuhara, T. Maki and N. Hansen: *Acta Mater.*, **54** (2006), 5323.
15) S. Morito, H. Yoshida, T. Maki and X. Huang: *Mater. Sci. Eng. A*, **438**–**440** (2006), 237.
16) K. Tsuzaki and T. Maki: *J. Jpn. Inst. Met.*, **45** (1981), 126.
17) S. Morito, R. Igarashi, K. Kamiya, T. Ohba and T. Maki: *Mater. Sci. Forum*, **638**–**642** (2010), 1459.
18) Y. Toji, T. Yamashita, K. Nakajima, K. Okuda, H. Matsuda, K. Hasegawa and K. Seto: *ISIJ Int.*, **51** (2011), 818.
19) T. Maki, K. Tsuzaki and I. Tamura: *Trans. Iron Steel Inst. Jpn.*, **20** (1980), 207.
20) S. Morito, J. Nishikawa, T. Ohba, T. Furuhara and T. Maki: Proc. ICOMAT 2008, ed. by G. B. Olson, D. S. Liberman, A. Saxena, TMS, PA, (2009), 649.
21) N. Sato, Y. Adachi, H. Kawata and K. Kaneko: *ISIJ Int.*, **52** (2012), 1362.